Brain Structure and Function
https://doi.org/10.1007/s00429-017-1575-z

ORIGINAL ARTICLE

Repeated shock stress facilitates basolateral amygdala synaptic plasticity through decreased cAMP-specific phosphodiesterase type IV (PDE4) expression

Steve Ryan[1,2] · Chenchen Li[1,2] · Aurélie Menigoz[1,2] · Rimi Hazra[3] · Joanna Dabrowska[4,5] · David Ehrlich[6,7] · Katelyn Gordon[1] · Donald G. Rainnie[1,2]

Received: 22 December 2016 / Accepted: 7 November 2017

Abstract

Previous studies have shown that exposure to stressful events can enhance fear memory and anxiety-like behavior as well as increase synaptic plasticity in the rat basolateral amygdala (BLA). We have evidence that repeated unpredictable shock stress (USS) elicits a long-lasting increase in anxiety-like behavior in rats, but the cellular mechanisms mediating this response remain unclear. Evidence from recent morphological studies suggests that alterations in the dendritic arbor or spine density of BLA principal neurons may underlie stress-induced anxiety behavior. Recently, we have shown that the induction of long-term potentiation (LTP) in BLA principal neurons is dependent on activation of postsynaptic D1 dopamine receptors and the subsequent activation of the cyclic adenosine 5′-monophosphate (cAMP)—protein kinase A (PKA) signaling cascade. Here, we have used in vitro whole-cell patch-clamp recording from BLA principal neurons to investigate the long-term consequences of USS on their morphological properties and synaptic plasticity. We provided evidence that the enhanced anxiety-like behavior in response to USS was not associated with any significant change in the morphological properties of BLA principal neurons, but was associated with a changed frequency dependence of synaptic plasticity, lowered LTP induction threshold, and reduced expression of phosphodiesterase type 4 enzymes (PDE4s). Furthermore, pharmacological inhibition of PDE4 activity with rolipram mimics the effects of chronic stress on LTP induction threshold and baseline startle. Our results provide the first evidence that stress both enhances anxiety-like behavior and facilitates synaptic plasticity in the amygdala through a common mechanism of PDE4-mediated disinhibition of cAMP-PKA signaling.

Keywords Macromolecular complexes · Compartmentalization · a-Kinase anchoring protein · Basolateral amygdala · Chronic stress · Morphology

Steve Ryan and Chenchen Li contributed equally to this work.

✉ Donald G. Rainnie
drainni@emory.edu

1 Behavioral Neuroscience and Psychiatric Disorders, Yerkes National Primate Research Center, Atlanta, GA, USA

2 Department of Psychiatry, Emory University School of Medicine, Atlanta, GA, USA

3 Department of Medicine, Center for Translational and International Hematology, Vascular Medicine Institute, University of Pittsburgh, Pittsburgh, PA, USA

4 Department of Cellular and Molecular Pharmacology, Chicago Medical School, Rosalind Franklin University of Medicine and Science, North Chicago, USA

5 Department of Neuroscience, Chicago Medical School, Rosalind Franklin University of Medicine and Science, North Chicago, USA

6 Department of Neuroscience and Physiology, Neuroscience Institute, NYU Langone Medical Center, New York, NY, USA

7 Department of Otolaryngology, NYU Langone School of Medicine, New York, NY, USA

Published online: 04 December 2017

Introduction

Chronic stress has been associated with precipitation of anxiety, depression, and other mood-related disorders. Great therapeutic potential, therefore, exists in identifying the molecular mechanisms encoding the effects of chronic stress in the brain. Previous studies have shown that exposure to acute or chronic stressful events facilitates memory formation in classical conditioning tasks, including fear conditioning (Shors et al. 1992; Beylin and Shors 1998; Cordero et al. 2003), and fear memory (Rau et al. 2005; Rodriguez Manzanares et al. 2005). The basolateral amygdala (BLA) is a key site that mediates the formation of fearful memories (LeDoux 1993; Rogan et al. 1997; Blair et al. 2001). Clinical evidence indicates that stress-related affective disorders are associated with a higher level of basal activity in the basolateral amygdala (BLA) (Abercrombie et al. 1998; Drevets 1999) and exaggerated responses to fearful stimuli (Rauch et al. 2000; Villarreal and King 2001). Experimental evidence in rodents is consistent with this presentation, showing that stress causes hyperexcitability (Rosenkranz et al. 2010) and enhances synaptic connectivity (Vyas et al. 2006) in the rat BLA. Moreover, exposure to acute stress facilitates synaptic plasticity in the BLA (Rodriguez Manzanares et al. 2005; Vouimba et al. 2004). Together this evidence indicates that exposure to stress can enhance fear and anxiety-like behavior as well as facilitate synaptic plasticity in the BLA, but the cellular mechanisms which mediate those responses remain unclear.

Our lab has recently shown that the induction of long-term potentiation (LTP) in BLA principal neurons is dependent on activation of postsynaptic D_1 dopamine receptors and the subsequent activation of the cAMP-PKA signaling cascade (Li et al. 2011). We have also shown that D_1 receptors are enriched in the spines of BLA principal neurons where they interact directly with NMDA receptors to facilitate synaptic plasticity (Pickel et al. 2006). One of the enzymes critical to controlling the intracellular concentration of cAMP is the phosphodiesterase 4 family (PDE4), a large family of enzymes that includes the PDE4A, B, C, and D subtypes, which convert cyclic AMP to linear 5′-AMP. Evidence suggests PDE4s act as a high-affinity sink for cAMP, preventing unfettered diffusion and leading to tightly compartmentalized cAMP signaling (Baillie and Houslay 2005; Li et al. 2009; Terrin et al. 2006). This is enabled by the macromolecular complex PDE4s associate with, including A-kinase-anchoring protein, DISC1, and β-arrestin, which collaborate to control the dynamics of cAMP signaling in dendritic spines. As a result, PDE4s are perfectly situated to mediate stress-induced alterations to synaptic plasticity and behavior. Interestingly, PDE4D knock out animals show enhanced LTP and impaired learning using a conditioned fear paradigm (Rutten et al. 2008), whereas PDE4B knock out animals shows enhanced long-term depression (LTD), impaired reversal learning in the Morris water maze, and an anxiety-like phenotype (Rutten et al. 2011; Zhang et al. 2008).

Recent studies have suggested that alterations to dendritic morphology and spine density in the BLA may underlie the stress-induced changes of anxiety behavior and synaptic plasticity (Mitra et al. 2005; Vyas et al. 2002). In this study, we have performed detailed morphological reconstructions of individual physiologically identified BLA principal neurons to provide a new perspective on this hypothesis, and built on our previous work on molecular mechanisms in BLA plasticity to explore the hypothesis that PDE4s may play a role in regulating the effects of stress on synaptic plasticity and anxiety behavior.

Methods

Animals

Sprague–Dawley rats were group housed, kept on an artificial 12:12-h light cycle, kept at 22 °C, and given access to water and food ad libitum. All experimental protocols conform to the National Institutes of Health Guidelines for the Care and Use of Laboratory Animals, and were approved by the Institutional Animal Care and Use Committee of Emory University.

Slice physiology

To enable neuronal reconstructions at each time point, we performed whole-cell patch-clamp to identify BLA principal neurons based on electrophysiological properties as described previously (Ehrlich et al. 2012) and to visualize neurons, biocytin (0.35%, Sigma–Aldrich, St Louis, MO, USA) was included in the patch recording solution. Acute brain slices containing the BLA were obtained as previously described (Rainnie 1999). Briefly, animals were decapitated under isoflurane anesthesia (Fisher Scientific, Hanoverpark, IL, USA). Then the brains were rapidly removed and immersed in ice cold "cutting solution", perfused with 95%-oxygen/5%-carbon dioxide gas and composed of (in mM): NaCl (130), NaHCO3 (30), KCl (3.50), KH2PO4 (1.10), MgCl2 (6.0), CaCl2 (1.0), glucose (10), ascorbate (0.4), thiourea (0.8), sodium pyruvate (2.0), and kynurenic acid (2.0). Slices were prepared at 350 µm using a Leica VTS-1000 vibrating-blade microtome (Leica Microsystems Inc., Bannockburn, IL, USA). Slices were kept in oxygenated cutting solution at 32 °C for 1 h before transferring

to regular artificial cerebrospinal fluid (ACSF) containing (in mM): NaCl (130), NaHCO3 (30), KCl (3.50), KH2PO4 (1.10), MgCl2 (1.30), CaCl2 (2.50), glucose (10), ascorbate (0.4), thiourea (0.8) and sodium pyruvate (2.0), at room temperature.

Patch-clamp recording

Individual slices were transferred to a submersion-type recording chamber mounted on the fixed stage of a Leica DM6000 FS microscope (Leica Microsystems Inc., Bannockburn, IL, USA), and continuously perfused by gravity-fed oxygenated 32 °C ACSF at a flow rate of 1–2 ml/min. Slices were viewed using differential interference contrast (DIC) optics and infrared (IR) illumination with an IR sensitive CCD camera (Orca-flash2.8, Hamamatsu, Tokyo, Japan). Thin-walled borosilicate glass patch electrodes (WPI, Sarasota, FL, USA), which had a resistance of 4–6 MΩ, were filled with a patch solution containing (in mM): K^+-gluconate (130), KCl (2), HEPES (10), $MgCl_2$ (3), K-ATP (2), Na-GTP (0.2), and phosphocreatine (5), adjusted to pH 7.3 with KOH, and having an osmolarity of 280–290 mOsm. Individual BLA projection neurons were visualized in situ using DIC microscopy in combination with a 40x water immersion objective and displayed in real time on a computer monitor. Projection neurons were identified according to their characteristic size and shape (Rainnie et al. 1993), and were normally located between 50 and 120 µM beneath the surface of the slice. Data acquisition and analysis were performed using a MultiClamp700B amplifier in conjunction with pClamp 10.2 software and a DigiData 1320A AD/DA interface (Molecular Devices (MDC), Sunnyvale, CA, USA). Whole-cell patch-clamp recordings were obtained and recorded voltages were low-pass filtered at 5 kHz and digitized at 10–20 kHz. At the start of each experiment, a series of standardized current clamp protocols were performed to validate the identity of BLA projection neurons.

To examine the frequency–response curve of synaptic plasticity in BLA projection neurons, pharmacologically isolated excitatory postsynaptic potentials (eEPSPs) were evoked as previously described (Li et al. 2011; Braga et al. 2004). In brief, a concentric bipolar stimulation electrode (FHC, Bowdoinham, ME, USA) was placed approximately 500 µm from the recorded neuron, close to the fiber tract of the external capsule immediately adjacent to the BLA (Fig. 3a). In all experiments, 50 µM picrotoxin was added to the patch solution to block $GABA_A$ currents exclusively in the recorded neuron. In addition, slices were continuously perfused with oxygenated ACSF (32 °C) containing the $GABA_B$ receptor antagonist CGP36742 (2 µM). This recording configuration allowed stable recording of isolated EPSPs without contamination from epileptiform, recurrent EPSPs.

EPSPs were evoked at 0.05 Hz and adjusted to 30% of the maximal response, and those eEPSPs obtained 10 min immediately before drug treatment were considered as baseline. All EPSPs evoked during and after treatments were normalized to the mean baseline amplitude and expressed as a percentage of baseline amplitude. For LTD and LTP experiments, recordings continued for at least 40 min after the induction protocol terminated. The protocols used to induce LTD were: low-frequency stimulation (LFS) using 900 stimuli at 1 Hz. As previously reported, LTP was induced using a 5×100 Hz protocol, which consisted of five trains of stimulation at 100 Hz for 1-s duration, applied at 20 s intervals. A 2×100 Hz protocol was used as a subthreshold protocol to examine the effects of drug treatment on LTP threshold (Li et al. 2011). Intermediate stimulation frequencies consisted of 900 stimulation pulses at 5, 10, and 30 Hz. A DC holding current was injected to maintain the membrane potential at − 70 mV, except during HFS when the potential was adjusted to − 60 mV.

Morphological reconstructions

A subset of patched neurons were labeled with biocytin (Sigma–Aldrich, St Louis, MO, USA) included in the patch pipette recording solution. Reconstructions and analysis were conducted as previously described (Ryan et al. 2014), but briefly: after neurons were recorded for at least 15 min, slices were fixed in 10% buffered formalin (Fisher Scientific, Hanoverpark, IL, USA) for 12–72 h, and then transferred to cryoprotectant for storage at − 20 C. Tissue was washed, permeabilized, and treated with Alexa Fluor 488-conjugated Streptavidin (Invitrogen, Grand Island, New York, USA) diluted to 1:1000 in PBS with Triton X-100 overnight at room temperature. Slices were then washed again and mounted on glass slides, air-dried, and cover-slipped with mowiol mounting medium (Sigma–Aldrich, St Louis, MO, USA).

For morphological analysis, the dendritic arbor of each neuron was first reconstructed by hand using Neurolucida neuron tracing software (MicroBrightField, Colchester, VT) from single *z* stack images taken at 10x magnification with a 0.4 µm step size using a Leica DM5500B spinning disk confocal microscope (Leica Microsystems Inc., Bannockburn, IL, USA) and SimplePCI data acquisition software (Compix, Sewickley, PA). Quantitative analysis of reconstructions was performed using Neurolucida Explorer (MicroBrightField). Dendritic length and branching were analyzed in Neurolucida Explorer using Sholl analyses with ring radius increments of 2 µm, and data were analyzed in Matlab (The MathWorks, Natick, MA, USA). To estimate the average spine density for BLA principal neurons, we manually counted

dendritic spines with Neurolucida on image stacks of dendrite segments taken at 100x magnification. For each neuron, spines were counted by a blinded experimenter on 10 non-overlapping dendritic segments. Each segment spanned 50 µm and was centered on 1 of 10 points in the dendritic arbor chosen pseudo-randomly by a custom Matlab script (available upon request), making the selections agnostic to branch order or distance from soma. All protrusions were counted as spines. Total spine number was estimated for each neuron individually using the product of average spine density and aggregate dendritic length, defined as the sum of the lengths of all dendritic segments.

Acoustic startle test

In the acoustic startle response (ASR), rats were placed in an acoustic startle chamber for 5 min prior to testing to acclimatize the animals to the chambers. Four rats were tested simultaneously in identical 8 × 15 × 15 cm Plexiglas and wire mesh cages, each suspended between compression springs within a steel frame located within a custom-designed sound attenuating chamber. Details of the recording apparatus have been reported previously [Sink et al., 2011; Walker and Davis 1997]. Subsequently, the ASR was measured following each of 30 acoustic stimuli. Startle responses were evoked by 50-ms 100, 105 and 110 dB white-noise bursts generated in a pseudorandom order by a Macintosh G3 computer sound file, amplified by a Radio Shack amplifier (100 W, Model MPA-200; Tandy, Fort Worth, TX, USA), and delivered through speakers located 5 cm in front of each cage. Startle amplitude was defined as the maximum peak-to-peak voltage of the Instrument's output during the first 200 ms after each noise burst. The presentation and sequencing of all stimuli was under the control of a Macintosh G3 computer using custom-designed software (The Experimenter; Glassbeads Inc., Newton, CT, USA).

Repeated stress procedure and behavioral analysis

Details of the USS paradigm used in these experiments (Fig. 1a) were adapted from previous studies in rat and human (Walker et al. 2003; Moberg and Curtin 2009) and have been reported previously (Hazra et al. 2012). Before administering the USS, rats, 35 days of age, were first matched for their basal anxiety level using a standard acoustic startle paradigm (see above). Animals were then divided into two cohorts of 8 animals according to their initial startle response, 8 NS rats and 8 USS rats. NS animals received exactly the same handling procedures as the USS group and were placed in the shock chamber for the same duration without being shocked.

On day 1, the USS rats were placed in the shock chamber and allowed to habituate to their environment for 5 min. Rats then received two 8-min periods of eight randomly applied footshocks (0.5 s, 0.5 mA) separated by an 8-min period of no shock. The USS paradigm was repeated on each of the following 3 days for a total of 4 consecutive days of shock stress. Each rat was shocked at approximately the same time every day (10 a.m.) to control for diurnal hormone variations. Rats in both groups were then returned to their home cages for 6 days. On the 10th day, the rats were first measured for their post-stress startle response. All animals in this study received either the USS protocol or the sham NS protocol before being allocated to either electrophysiological or genetic experiments. Animals allocated for electrophysiology experiments were used equally to collect samples for dendritic morphology and synaptic plasticity to distribute variance more evenly among animals.

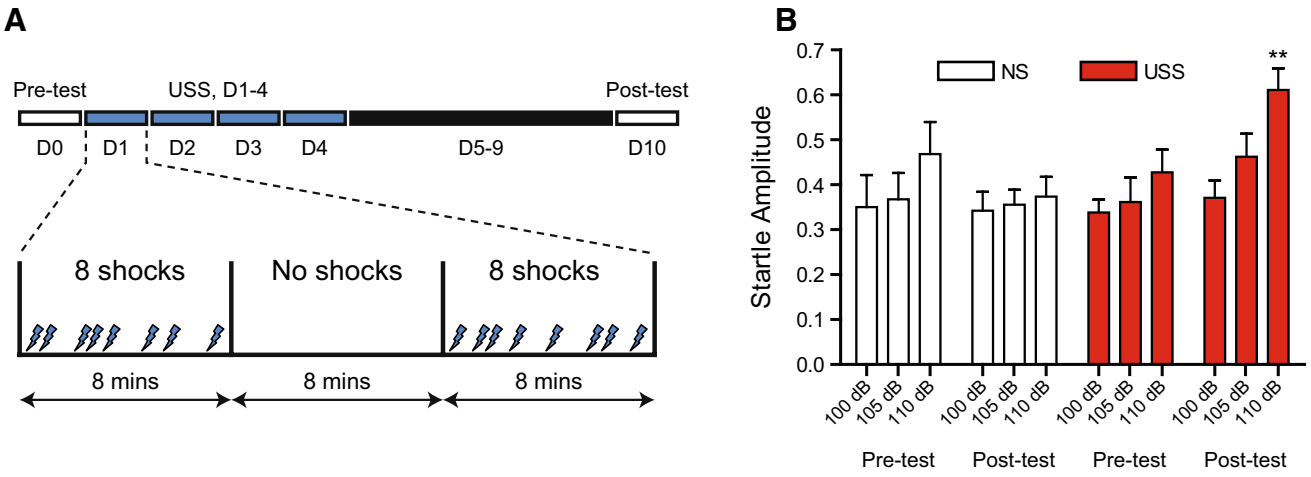

Fig. 1 4 days of unpredictable shock stress rats leads to heightened anxiety. **a** Schematic of unpredictable shock stress paradigm, including acoustic startle pre- and post-tests, and 4 days of USS. **b** USS rats show increase in acoustic startle amplitude from pre-test to post-test

Surgery

Rats (weighing 150–200 g when surgery began) were anesthetized with isoflurane (2.5%). Guide cannula (C313G/SPC; Plastics One, Roanoke, VA) were bilaterally implanted 1 mm above the BLA. The coordinates for the BLA were anterior/posterior, − 2.7 mm; medial/lateral, ±5.0 mm; dorsal/ventral, − 7.9 mm. Glasslute cement was placed around the cannulae to hold each in place. Dental cement is then placed around the cannulae and screws until a secure mound is formed, which is given time to harden. A stainless-steel stylet blocker was inserted into each cannula to keep them patent and prevent infection. The rats were allowed to recover for 5–7 days after surgery.

Drugs and infusion procedure

Rolipram (0.1 mg/ml) was prepared fresh on the day of infusion in sterile ACSF vehicle. Injection cannulae (36 gauges) (Plastics One, model C313I/SPC) were used for bilateral BLA infusions (0.5 µl/min, 1 µL total volume/side); after the infusions were completed, the injection cannulae were left in place for 2 min to allow for diffusion, where upon the stylets were placed back into the guide cannula. The dose of rolipram (0.1 mg/ml, 1 µl/side) was based on previous studies of intra-amygdala CGRP effects on fear-related behaviors. At the end of the experiments, the rats were killed by isoflurane overdose and perfused. Cannula placements were assessed using Nissl staining with a section thickness of 40 µm under light microscopy. Rats with misplaced cannulas were excluded from the statistical analysis.

Quantitative whole-tissue PCR

Whole BLA tissue was collected by microdissection from live brain slices harvested after decapitation under anesthesia, as previously described (Ehrlich and Rainnie 2015). Total RNA purification was performed using Trizol (ThermoFisher, CA) extraction. For the reverse transcription, RNA was incubated 5 min at 65 °C with 1 µl of oligodT 20 (50 mM) and 1 µl of dNTP (10 mM; Life Technologies, CA). After 1 min on ice 1 min, the reverse transcription mix was added (2 µl of RT buffer, 2 µl of MgCl 2 50 mM, 2 µl of DTT 0.1 M and 1 µl of SuperScript III enzyme; Life Technologies, CA). The cDNA synthesis was carried at 50 °C for 50 min, followed by 5 min at 85 °C for inactivation. The cDNA was then stored at − 20 °C until used.

To test the quality of the newly synthesized cDNA, control PCRs were performed using GAPDH as positive control. The PCR was performed according to standard protocol from manufacturer [HotStart Taq polymerase (Qiagen)], with 1 µl of cDNA for template. The results were visualized on 2% agarose gel with Ethidium bromide. For qPCR, the cDNA were pre-amplified using PreAmp mix (Thermofisher) and the combination of all the taqman assays for the genes of interest. Amplification reactions (20 µl), composed of 2 µl cDNA template (1/500), Universal TaqMan MasterMix (2x concentrated, Life Technologies), TaqMan assay (see Table 1; 20× concentrated, Life Technologies) and H2O, were performed with the 7500 Fast Real-Time PCR System (Life Technologies) in 96-well plates. Reactions were run in triplicate. Non-template controls were used as negative controls in every experiment. GAPDH and B2M, selected using the geNorm application, were used as endogenous controls for calibration. The relative expression of mRNA was normalized to the geometric mean of the calibrators, using the ΔCt method (Vandesompele et al. 2002; Livak and Schmittgen 2001).

Statistics

Behavior data pre-tests were compared using Students unpaired *t* test, two-tailed, between the control and USS group prior to group assignment to ensure that baseline startle was not significantly different. Following startle post-test, the groups were compared using two-way repeated measures ANOVA to assess effect of stress and noise amplitude. When comparing qPCR results, where variances were unequal between groups, non-parametric Mann–Whitney *U* tests were used to compare control and stress groups within gene, and adjusted for multiple comparisons. Significance of long-term potentiation or depression in plasticity experiments was tested by comparing the 10-min baseline to a 10-min window of measurements starting 30 min after the end of stimulation using a two-way ANOVA. Comparisons across groups of total plasticity were made between the same 10-min periods starting 30 min after stimulation.

Results

USS elicits a long-lasting increase in the baseline startle response in rats

Prior to receiving the unpredictable shock stress (USS), 16 rats were tested for their baseline acoustic startle in response to three different intensities of white noise, 100, 105, and 110 dB. The graded intensity allowed us

Table 1 Reference numbers for the Taqman assays used in qPCR experiments

Gapdh	Rn01775763_g1
B2m	Rn00560865_m1
PDE4A	Rn00565354_m1
PDE4B	Rn00566785_m1
PDE4D	Rn00690450_m1

to examine any alteration in the sensitivity to the startle stimulus resulting from the stress manipulation. Rats were then matched according to their startle response and placed in either the non-stress (NS) or the USS group. Consequently, at day 0 there was no significant difference in the mean startle amplitude (Fig. 1b, mean pre-test amplitude NS group = 0.39 ± 0.06 vs USS group = 0.38 ± 0.04, $n = 8$ respectively, $p > 0.05$). As illustrated in Fig. 1b, following USS, rats had a significantly increased startle response on day 10 when compared to pre-test that was not detected in age-matched litter mate controls (mean post-test amplitude NS group = 0.36 ± 0.04 vs USS group = 0.48 ± 0.05, two-way ANOVA, $F_{(2,30)} = 7.847$ $p < 0.01$). The startle response was enhanced significantly only at 110 dB levels tested (mean post-test amplitude USS pre-test = 0.42 ± 0.04 vs USS group = 0.61 ± 0.05). These results indicate that our USS protocol successfully induced a long-lasting increase in anxiety-like behavior.

USS does not affect the morphological properties of BLA projection neurons

Previous studies have shown that, in the hippocampus and amygdala, exposure to stress can lead to growth or retraction of the dendritic arbor in the principal neurons of these brain regions (Vyas et al. 2002). In this study, we took advantage of the whole-cell patch-clamp setup to fill individual physiologically identified BLA principal neurons with biocytin in both USS and NS animals, enabling detailed morphological reconstructions (Fig. 2a, representative reconstruction). We assessed total dendritic length of neurons in USS and NS animals and found no statistically significant difference (Fig. 2b; NS: 5677 ± 1558 µm, $n = 16$; USS: 6314 ± 1767 µm, $n = 15$, Student's unpaired t test, $p > 0.05$). In a subset of filled neurons, we used high-resolution 100× images to evaluate spine density ($n = 6$ cells per group), and found no significant difference (Fig. 2c; NS: 8357 ± 2447 µm; USS: 8925 ± 3172 µm, Student's unpaired t test, $p > 0.05$). Finally, we measured the distribution of dendritic material relative to the soma by conducting a Sholl analysis, and saw no significant difference (two-way ANOVA, $p > 0.05$).

USS-induced frequency-dependent changes in synaptic plasticity

We have previously shown that exposure to USS increases the frequency of spontaneous synaptic activity in BLA principal neurons (Hubert et al. 2014), as well as elicits a long-lasting enhancement in anxiety-like behavior. Moreover, previous studies have shown that stress causes hyperexcitability (Rosenkranz et al. 2010), and even facilitates synaptic plasticity in BLA (Rodriguez Manzanares et al. 2005; Vouimba et al. 2004). We, therefore, investigated whether synaptic

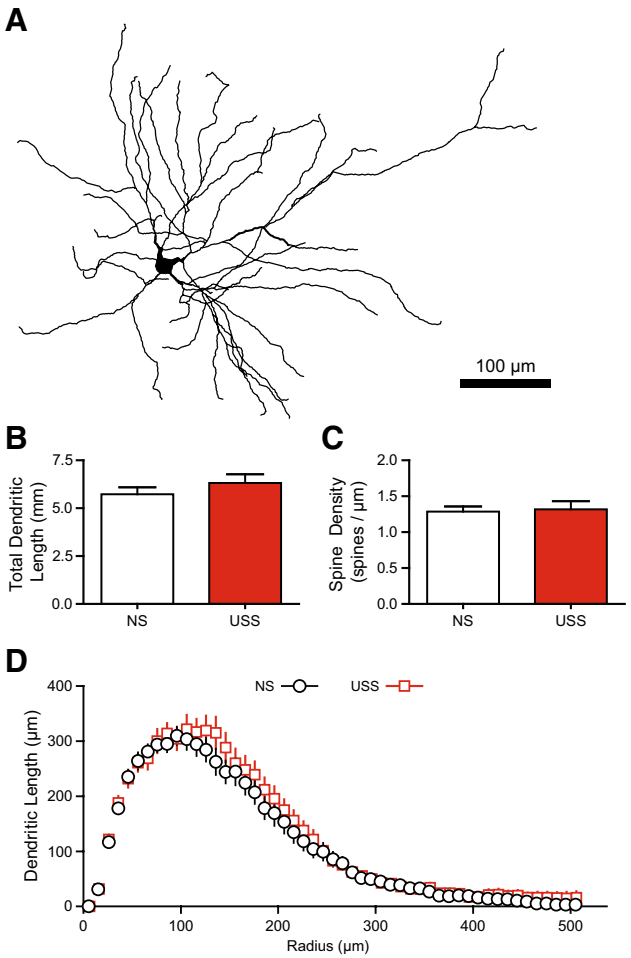

Fig. 2 Chronic stress has no effect on dendritic morphology of BL A principal neurons. **a** Example reconstructed BLA principal neuron. **b–d** No effect of chronic stress on total dendritic length (**b**), spine density (**c**), or distribution of dendritic material with respect to the cell body (**d**)

plasticity induced by a variety of different stimulation protocols might change in the BLA slices derived from NS vs USS animals. The stimulus-evoked excitatory postsynaptic potential (eEPSP) in BLA projection neurons was recorded following stimulation of the external capsule (EC). For these studies, monosynaptic eEPSPs were examined in isolation following blockade of $GABA_A$ receptor-mediated synaptic transmission (see "Methods"). The peak amplitude of eEPSP was measured and normalized to mean peak eEPSP amplitude for the 10 min baseline period before the LTP- or LTD-induction protocol.

As shown in Figs. 3b, a, 5× high frequency stimulation (HFS; 5 1-s trains at 100 Hz at 20 s intervals) induced a significant and robust LTP of the eEPSP that lasted for > 45 min in slices from both NS and USS animals (Fig. 3b; NS: 155 ± 13% of baseline 30 min after HFS, $n = 6$, 4 animals, black circles, $p < 0.0001$; USS: 163 ± 14% of baseline

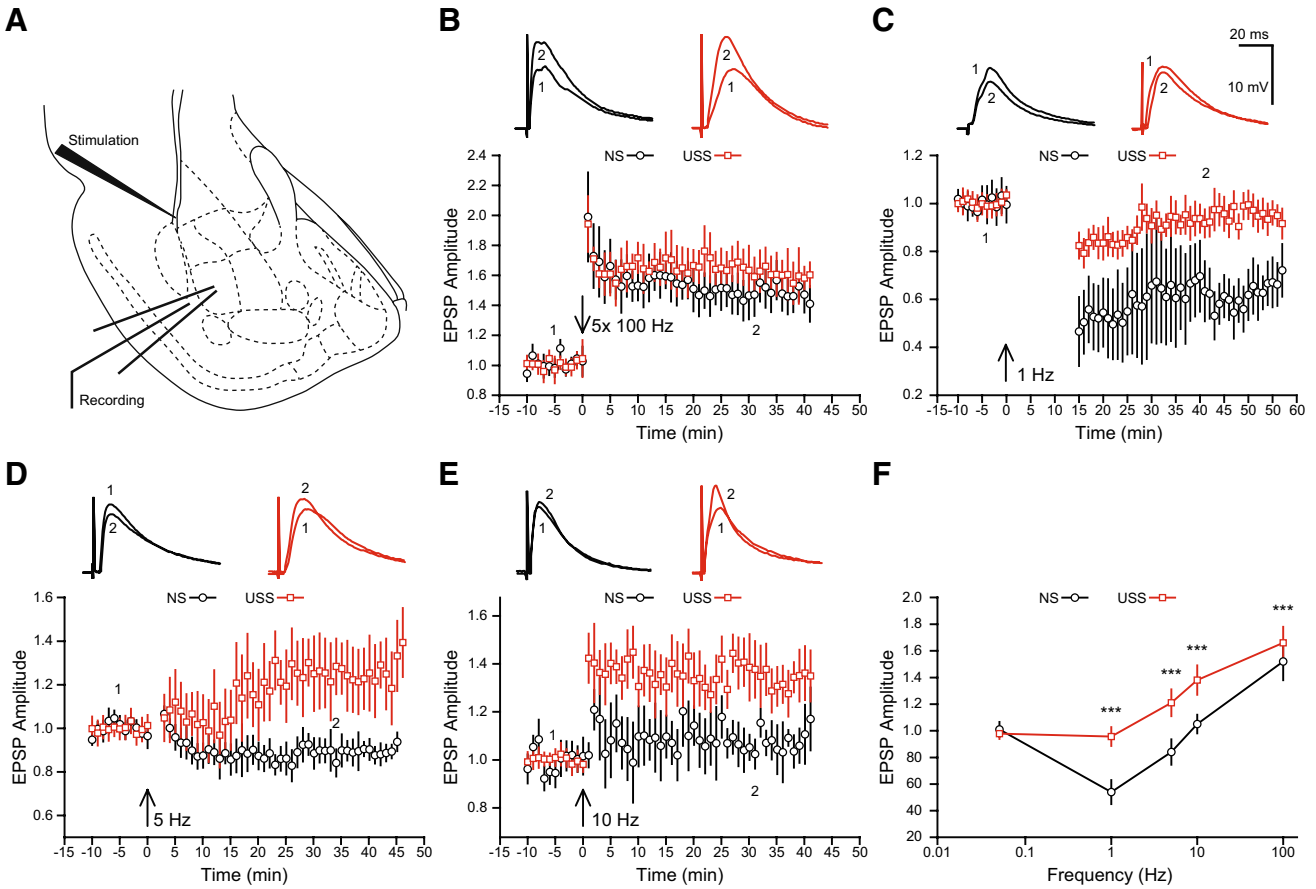

Fig. 3 Chronic stress enhances LTP generated by HFS and abolishes LTD generated by LFS. **a** Experimental schematic showing stimulation of the external capsule and recording from BLA. **b**–**e** Synaptic stimulation at different frequencies shows a spectrum of potentiation and depression in non-stress animals which is altered by exposure to chronic stress. A summary of the effects on synaptic plasticity is shown in (**f**), with asterisks indicating comparisons between stress and non-stress groups after 30 min

30 min after HFS, $n=6$, 4 animals, red squares, $p<0.0001$). We next examined the response of BLA projection neurons to low-frequency stimulation of the EC (1 Hz, 900 pulses), a protocol which is known to induce stable LTD in slices from NS animals (61.4 ± 8%, $n=6$, 4 animals, Fig. 3c, black circles). Intriguingly, BLA projection neurons from USS animals exhibited a significant reduction in LTD compared to NS animals (95.7 ± 7%, $N=6$, 4 animals, Fig. 3c, red squares, $p<0.0001$). These experiments revealed deficits in synaptic plasticity in BLA slices from the USS animals. Hence, we next explored the frequency–response curve for LTD–LTP induction in NS and USS animals. Slices were stimulated using other low-frequency stimulation patterns (900 stimuli at 5 or 10 Hz), to see if the transition from LTD to LTP is altered in the USS slices, and at what frequency or time point. As shown in Fig. 3d, in NS animals 5 Hz stimulation induced a small but noticeable LTD (89.7 ± 5%, $n=7$, 4 animals, Fig. 3D, black circles, $p<0.0001$). In contrast, no LTD was observed in BLA projection neurons from USS animals, and 15 min after stimulus offset there was a small amount of LTP (124 ± 19% of baseline, $n=5$, 3 animals, $p<0.0001$, Fig. 3d, red squares). In slices from NS animals, 10 Hz stimulation had no significant net effect on the amplitude of the eEPSP (102 ± 6%, $n=5$, 3 animals, Fig. 3e, black circles), whereas a long-lasting LTP was induced by 10 Hz stimulation in BLA projection neurons in USS animals (138 ± 12% of baseline, $n=5$, 3 animals, $p<0.0001$, Fig. 3e, red squares). The LTD–LTP frequency–response curves for NS and USS animals are summarized in Fig. 3f. As illustrated, USS results in a significant leftward shift in the frequency response for LTP induction, and an apparent loss in LTD induction.

USS modulates the threshold of LTP induction in BLA principal neurons

We have shown that the LTP induced by 5xHFS was not changed in BLA projection neurons from USS animals; however, the stimulation frequency necessary for LTP induction in USS animals' slices was lower than in NS animals. Hence,

we next examined whether USS could affect the threshold for LTP induction in BLA using a sub-threshold stimulation protocol (2 1-s trains at 100 Hz at 20 s intervals; 2xHFS) (Li et al. 2011), which routinely fails to induce LTP in BLA projection neurons in NS animals (101 ± 7% of baseline, $n = 8$; Fig. 4a, black circles). Interestingly, 2xHFS induced a significant and sustained LTP in BLA principal neurons from rats exposed to USS (147 ± 13%, $n = 6$, $p < 0.0001$, Fig. 4b, red squares). Since we have shown that endogenous dopamine release and the subsequent activation of D_1 dopamine receptors are necessary for LTP induction in BLA principle neurons (Li et al. 2011), to test if the stress-facilitated LTP also needs endogenous dopamine release and D_1 receptor activation, slices collected from stressed animals were pretreated with the D_1 receptor antagonist SCH23390 for 10 min before 2xHFS stimulation. The effect of stress to reduce LTP induction threshold was fully blocked by prior application of SCH23390 (103 ± 9% of baseline, $n = 5$, 3 animals, $p < 0.05$, USS vs USS + SCH23390; Fig. 4c). These results suggest that USS results in increased excitability in BLA principal neurons, which in turn, facilitates the induction of LTP and that the lowered threshold of LTP induction still required endogenous dopamine release and the subsequent D_1 receptor activation.

Having confirmed the necessity of D_1 receptor activation in mediating the facilitating effect of USS on LTP induction, we next identified the possible signaling components that couple the D_1 receptor activation and the downstream cascade to exert USS effect. As we have shown that the activation of the cAMP-PKA cascade was required for the induction and maintenance of LTP in BLA principal neurons (Li et al. 2011), we investigated the possibility that the D_1 receptor-mediated activation of cAMP-PKA cascade was essential for USS-facilitated LTP induction. To test this possibility, we first examined the effect of USS on the LTP induction by inclusion in the patch pipette of the PKA inhibitor KT5720 (100 nM). Intracellular application of KT5720 significantly attenuated 2xHFS-induced LTP in BLA principal neurons from USS animals (105 ± 7% of baseline, $n = 5$, 4 animals, $p < 0.05$, USS vs USS + KT5720; Fig. 4c). These results suggest that the excitatory effect of USS on BLA LTP induction may due to a facilitation of the of cAMP-PKA signaling cascade. Two basic mechanisms could contribute to the facilitation of the cAMP-PKA signaling cascade; (1) the regulatory protein inhibitor-1, which in its phosphorylated form inhibits protein phosphatase-1 (PP1) could be upregulated (Blitzer et al. 1995, 1998; Otmakhova et al. 2000), or the metabolism cAMP to AMP may be downregulated and thereby contribute to USS-induced facilitation of LTP induction in BLA principal neurons. However, intracellular application of the broad spectrum PP1/2A inhibitor, okadaic acid (1 μM), failed to reduce the threshold for LTP induction in response to 2xHFS (116 ± 12% of baseline, $n = 6$, 4 animals, Fig. 4c).

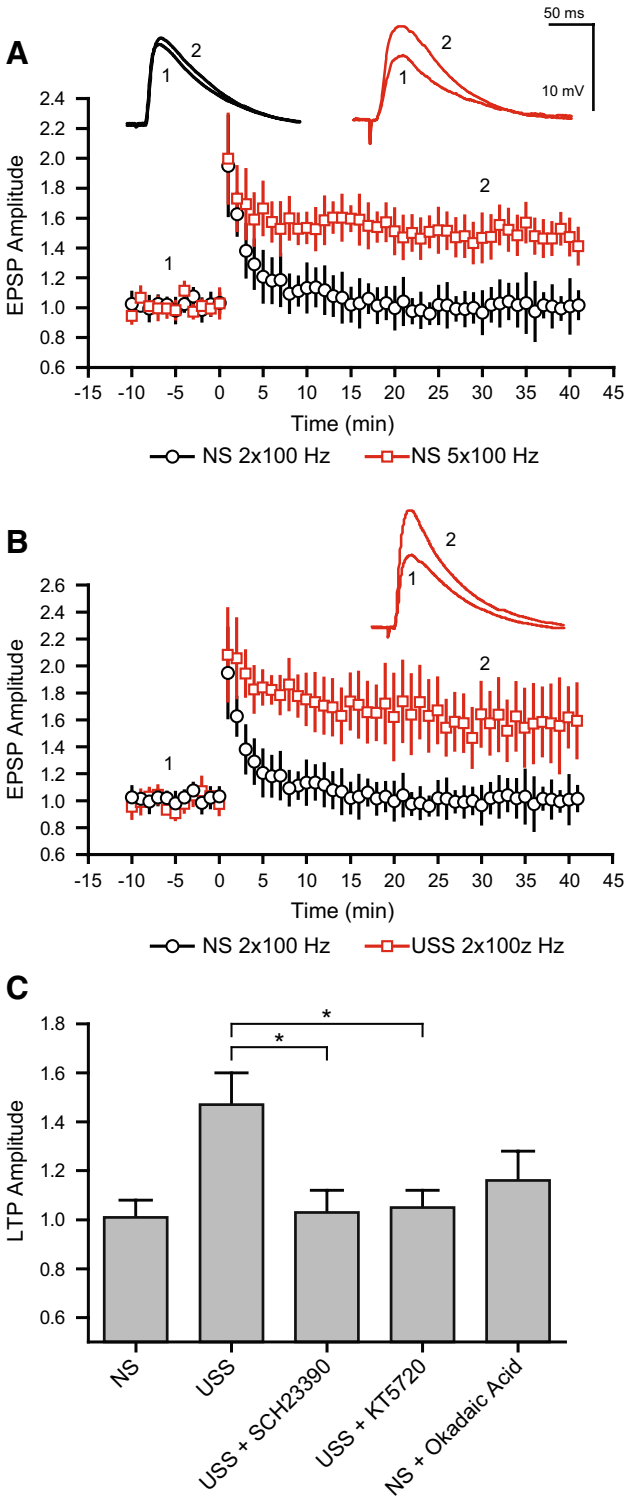

Fig. 4 Threshold for potentiation is lowered by exposure to chronic stress. In non-stress animals, the 2×100 Hz stimulation protocol is subthreshold for generating LTP (**a**), but produces substantial potentiation in stressed animals (**b**). **c** Enhanced LTP in stressed animals is still dependent on cAMP-PKA-dependent pathways as has been previously established

Consequently, we next investigated the relative contribution of the PDE4 family to the induction of LTP.

Inhibition of PDE4 lowered the threshold of LTP induction in BLA principal neurons

Here, we used whole-cell dual patch-clamp recordings (Fig. 5a) to investigate if application of the specific PDE4 inhibitor rolipram mimics the effect of USS on LTP induction in BLA principle neurons. Consistent with this hypothesis, intracellular application of low concentration of rolipram (100 nM) to only one of the pair of cells simultaneously recorded led to a reduced threshold for LTP induction in response to 2xHFS (153 ± 7% of baseline, $n = 6$, $p < 0.0001$, 3 animals, Fig. 5b), whereas the cell without rolipram application failed to show LTP induction (107 ± 9% of baseline, $n = 7$, 3 animals, Fig. 5b, significantly reduced from rolipram $p < 0.0001$). Similar to the USS condition, this enhanced LTP could be almost fully blocked by pretreatment with the D_1 receptor antagonist SCH23390 (10 µM) (114 ± 7% of baseline, $n = 6$, 2 animals, Fig. 5c).

USS down-regulates the mRNA expression of PDE4 isoforms to decrease cAMP degradation in BLA

The preceding results indicate that the excitatory effect of USS on LTP induction in BLA principal neurons may arise from a reduction of the metabolism of cAMP to AMP. The critical class of molecules responsible for this metabolic reaction are the PDE4s, known to be active in the BLA (Bureau et al. 2006). To determine whether the USS affects the cAMP metabolism, which in turn could contribute to the facilitation of LTP induction, we next investigated whether the USS paradigm affected PDE4 gene expression in the BLA.

Here, we used quantitative polymerase chain reaction (qPCR) to assess transcript expression for the major families of PDE4 expressed in the BLA—PDE4A, B, and D. We found that the majority of PDE4 transcript expression in control animals are in the PDE4 B & D families, and that expression of these is significantly reduced in USS-exposed animals (Fig. 6; $p < 0.001$; $n = 10$ animals in each group). Intriguingly, there was a low level of transcript expression of PDE4A in control animals, which was significantly increased following USS ($p < 0.001$).

Infusion of PDE4 inhibitor into BLA enhances the startle response

To determine whether diminished PDE4 activity in the BLA was sufficient to explain the increased anxiety displayed by USS animals, we infused rolipram into the BLA of control rats. Prior to receiving a rolipram infusion (0.1 mg/ml), 16 rats were tested for their baseline acoustic startle in response to 100, 105, and 110 dB white noise. Rats were then matched according to their startle response and placed in either the

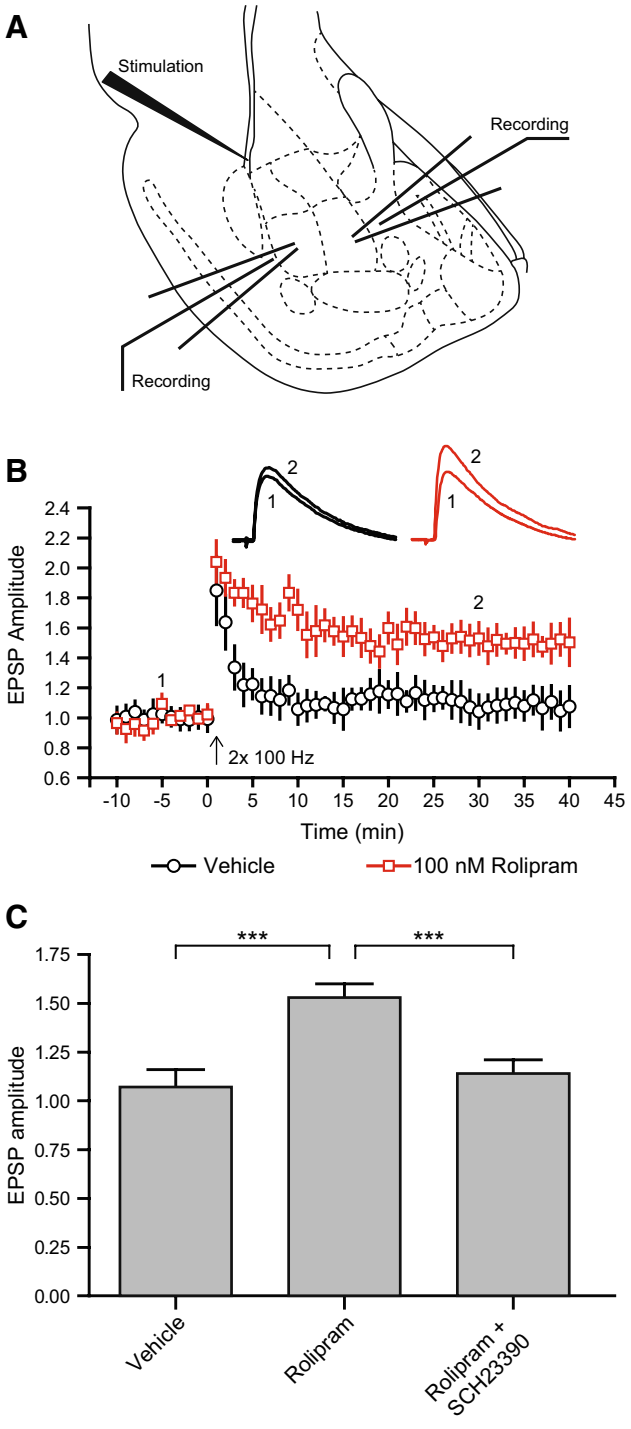

Fig. 5 Inhibition of PDE4 activity recapitulates the effects of stress on LTP threshold. Paired, simultaneous recordings of BLA principal neurons (**a**) in which one patch pipette contains rolipram, a PDE4 inhibitor, reduces the LTP threshold (**b**), similar to stressed animals. **c** Rolipram-induced reduction in LTP threshold is also D1 dependent

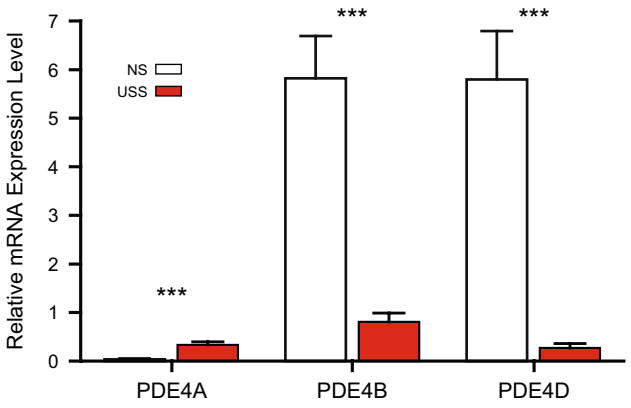

Fig. 6 Chronic stress radically alters expression of PDE4 subtypes B and D. Quantitative whole-tissue analysis of transcripts shows significant reduction in expression of PDE4B and D, and a small increase in expression of PDE4A

vehicle or the rolipram infusion group. For pre-test there was no significant difference in the mean startle amplitude (Fig. 7b, mean pre-test amplitude of 110 dB vehicle group = 0.47 ± 0.06 vs rolipram group = 0.43 ± 0.05, $n = 8$ respectively, two-way repeated measures ANOVA, $p > 0.05$). As illustrated in Fig. 7c, following rolipram infusion for 1 h, rats had a significantly increased startle response compared to vehicle group (mean 1 h post-test amplitude of 110 dB vehicle group = 0.37 ± 0.04 vs mean 1 h post-test amplitude rolipram group = 0.61 ± 0.04, two-way repeated measures ANOVA, $F_{(1,20)} = 7.961$, $p < 0.05$). The increased startle response appeared elevated at the highest decibel level after 24 h, but the effect did not reach the threshold for significance (mean 24 h post-test amplitude of 110 dB vehicle group = 0.39 ± 0.05 vs mean 24 h post-test amplitude rolipram group = 0.54 ± 0.08, two-way repeated measures ANOVA, $p > 0.05$, Fig. 7d). These results indicate that bilateral infusion of rolipram into BLA caused a significant, and long-lasting, enhancement of anxiety-like behavior.

Discussion

In this study, we have shown that USS increases anxiety-like behavior in rats and is associated with facilitation of LTP induction and no significant dendritic remodeling of BLA principal neurons. Specifically, we explored the effects of USS on dendritic morphology and showed that the effects of stress on dendritic morphology are non-significant and unlikely to explain the substantial behavioral responses known to follow chronic stress manipulations. In contrast, we also explored the effects of chronic stress on neuronal physiology, showing that the activity threshold necessary to produce LTP was significantly reduced in both frequency (Fig. 3) and intensity (Fig. 4) to such an extent that LTD normally produced by low-frequency stimulation is fully occluded in USS animals. Furthermore, our data show that the facilitated LTP still required the activation of dopamine

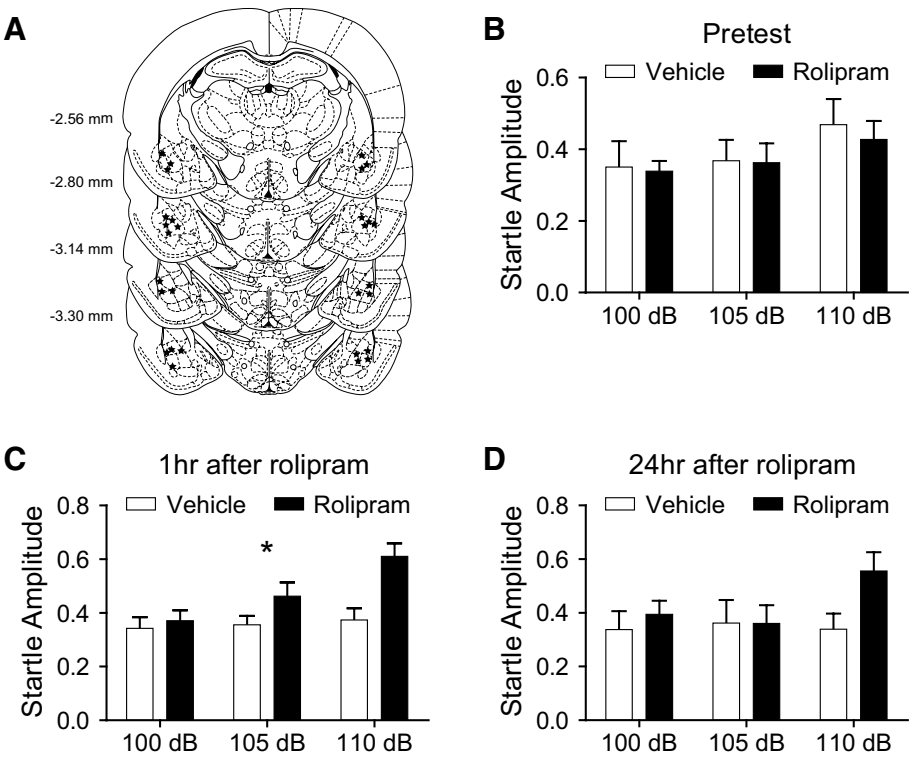

Fig. 7 Intra-BLA administration of rolipram produces a phenotype of enhanced anxiety. Injection sites identified by post hoc histology and illustrated in (**a**). Vehicle and rolipram animals show comparable anxiety in the pretest (**b**), but 1 and 24 h after infusion, rolipram animals show significantly enhanced stress at 110 dB

D_1 receptors, and was mediated through the cAMP-PKA signaling cascade. Finally, we have demonstrated that expression of PDE4 is dramatically reduced in USS animals, and that pharmacological inhibition of PDE4 can replicate the effects of stress on both synaptic plasticity and animal behavior. Our results support a plausible mechanism by which USS leads to enhanced LTP through down-regulation of PDE4, leading to amplified cAMP signals and a shift in the balance of synaptic plasticity towards potentiation.

Effects of chronic stress on synaptic plasticity are mediated through PDE4

The function and physiology of the BLA are known to be sensitive to stress. Chronic stress leads to enhanced memory consolidation (Rodriguez Manzanares et al. 2005; Conrad et al. 1999; Wood et al. 2008), and acute stress has been shown to lead to enhanced fear learning (Rau et al. 2005), increased baseline synaptic amplitude (Vouimba et al. 2004; Kavushansky and Richter-Levin 2006), and a reduced threshold for LTP induction (Rodriguez Manzanares et al. 2005). Furthermore, we have previously shown that chronic stress increases the AMPA receptor expression in presumed BLA principal neurons (Hubert et al. 2014), which could further facilitate the induction of LTP and explain the stress enhancement of baseline synaptic amplitude. Here, we used a chronic stressor and confirmed the previous reports of reduced threshold for LTP induction, but interestingly did not observe any reduction in LTP amplitude in stressed animals compared to control animals. The reduction in LTP amplitude may, therefore, be a transient effect seen only shortly after acute stressors that does not persist in the face of chronic stress. In addition, we have extended this work to demonstrate broader changes to synaptic plasticity in the BLA, showing that stress alters the BLA to both facilitate synaptic potentiation and inhibit synaptic depression in principal neurons. A similar disruption of the LTP-to-LTD balance has been reported following genetic disruption of the postsynaptic density protein 95 (PSD-95) and brain angiogenesis inhibitor 1 (BAI1), both of which are believed to form macromolecular complexes with AMPA receptors and other scaffolding proteins in the spines of glutamatergic neurons (Migaud et al. 1998; Zhu et al. 2015). Hence, spine-specific alterations in postsynaptic signaling can play a significant role in regulating synaptic plasticity and thus memory formation.

Work in the hippocampus has shown stress-induced impairment of LTP at synapses in both CA1 and CA3 appears to be mediated, at least in part, by alterations to PDE4 expression or activity level (Chen et al. 2010; Shors et al. 1990). This stands in interesting contrast to our own results, which show that both stress-induced and pharmacological inhibition of PDE4s lead to an enhancement of LTP in the BLA, but an opposite valence in the response would be consistent with an emerging pattern in the literature. Previous studies on stress-induced changes in dendritic morphology, show atrophy in the hippocampus and hypertrophy in the amygdala (Watanabe et al. 1992a, b; Vyas et al. 2002), and further studies have illustrated contrasting effects of the antidepressant tianeptine on cellular physiology in amygdala vs hippocampal CA1 (Pillai et al. 2012).

Despite the enormous interest in the PDE4 family of molecules as a possible target for therapeutic drugs, relatively little work has been done to understand the response of this important class of molecules to stress. Our study is the first to show a reduction in expression of PDE4 subtypes in the BLA in response to chronic stress. While we examined only the top-level categorization of PDE4s into the A, B, and D subtypes, each of these subtypes comprises numerous isoforms with unique characteristics and expression profiles. Further work will be necessary to address the nuances of how stress affects these isoforms with the ultimate goal of identifying isoforms well-positioned to mediate the response to chronic stress without generating undesirable side effects.

Beyond the additional detail of the numerous isoforms, further work will also be necessary to characterize the temporal dynamics of the response of the PDE4 system to chronic stress. Earlier work in other brain regions has shown a biphasic time course of PDE4 in response to a stressor similar to our own. Itoh and colleagues demonstrated that, following 3 days of stress, there is a transient reduction in adenylyl cyclase activity, PDE4 activity, and available rolipram binding sites, followed by a longer-term increase in PDE4 activity and available binding sites (Itoh et al. 2003). Furthermore, supporting the argument of time-sensitivity is the work of Werenicz et al., who showed significant effects of rolipram administration on memory formation in highly time-dependent fashion. It is apparent that the role of PDE4 molecules in contributing to memory formation is highly dynamic and time-sensitive (Werenicz et al. 2012; Klussmann 2016).

Dendritic remodeling as a response to stress

Chronic stress has been shown to lead to atrophy of dendritic arbor in hippocampal pyramidal neurons in CA3 (Watanabe et al. 1992a, b; Conrad et al. 1999; McEwen 2005). This dendritic atrophy is consistent with reports of deficits in spatial memory tasks and spatial reasoning in animals exposed to chronic stress, and has been posited as a mechanism to explain these deficits. Later research extended the observation of dendritic atrophy in response to chronic stress to pyramidal neurons in layer II/III of the medial prefrontal cortex (mPFC), in this case consistent with deficits in extinction learning. Substantial attenuation was reported, particularly in higher order, distal regions of the apical dendrite in response to stressors

both severe (Cook and Wellman 2004; Liu and Aghajanian 2008; Radley et al. 2004) and mild (Brown et al. 2005). Atrophy of dendritic shafts and spines has even been shown to be sufficiently consistent and specific that loss of mature dendritic spines in mPFC correlates well with the severity of deficits in extinction learning (Moench et al. 2015).

Recently, this line of inquiry has been extended to examine potential morphological consequences of chronic stress on neurons in the amygdala. Several studies have now shown similar findings, an apparent hypertrophy of dendritic material on amygdala neurons assessed with Golgi-Cox staining (Vyas et al. 2002, 2004; Padival et al. 2013; Suvrathan et al. 2014; Cui et al. 2008; Tsai et al. 2014), yielding estimates for total dendritic material of around 1500–2000 µm in control animals, and 2000–2500 µm in stressed animals. Consistent with past work, the present Sholl analysis revealed a small but non-significant increase in dendritic material following stress, mostly between 100 and 200 µm from the cell soma. Overall, we found stress to cause a small, non-significant increase in dendritic material of approximately 500 µm, also similar to the magnitude of the effect seen in previous studies. However, the effect of stress was proportionally smaller (~8%) in the present study, given that the dendritic arbors were nearly 4 times larger (~6000 vs 1500–2000 µm), consistent with our past work (Ryan et al. 2014). We contend that earlier Golgi-based studies under-reported overall dendritic length, either from cell selection bias or because thinly slicing tissue removes the majority of the dendritic arbor, and consequently over-emphasize the effect of stress on dendritic morphology. Interestingly, previous work in mice with a loss-of-function mutation knocked into the PDE4B gene has shown increased spine density in both hippocampus and amygdala (McGirr et al. 2016); however, our own electron microscopy studies of dendritic spines in the BLA following stress found no effect of stress on spine number or morphology (Hubert et al. 2014). This leaves open the possibility that attenuation of PDE4 activity by itself is sufficient to elevate spine density, but in some circumstances, buffers against altered spine density through other mechanisms.

While many of the studies cited above employ stress paradigms of greater intensity or longer duration than ours, we believe it is unlikely that the relative intensity of stressors explains the effect size, as our stressor was notably sufficient to result in changes in affective behavior, and some of the earlier studies observed their effects using only mild (Brown et al. 2005), or even single, acute stressors (Cui et al. 2008).

Concluding remarks

Our study suggests that modulation of PDE4 activity plays a major role in the response of the BLA to chronic stress. PDE4 is well situated to mediate changes to cellular physiology; as the major group of enzymes responsible for breaking down cAMP in the BLA, the molecule plays a central role in regulating the compartmentalization of postsynaptic cAMP signals. PDE4s are bound to scaffolding proteins like the A-kinase anchoring proteins (AKAPs; Fig. 8), which tether PDE4s and PKA near cellular membranes. During active cAMP signaling, cAMP levels rise and activate PKA,

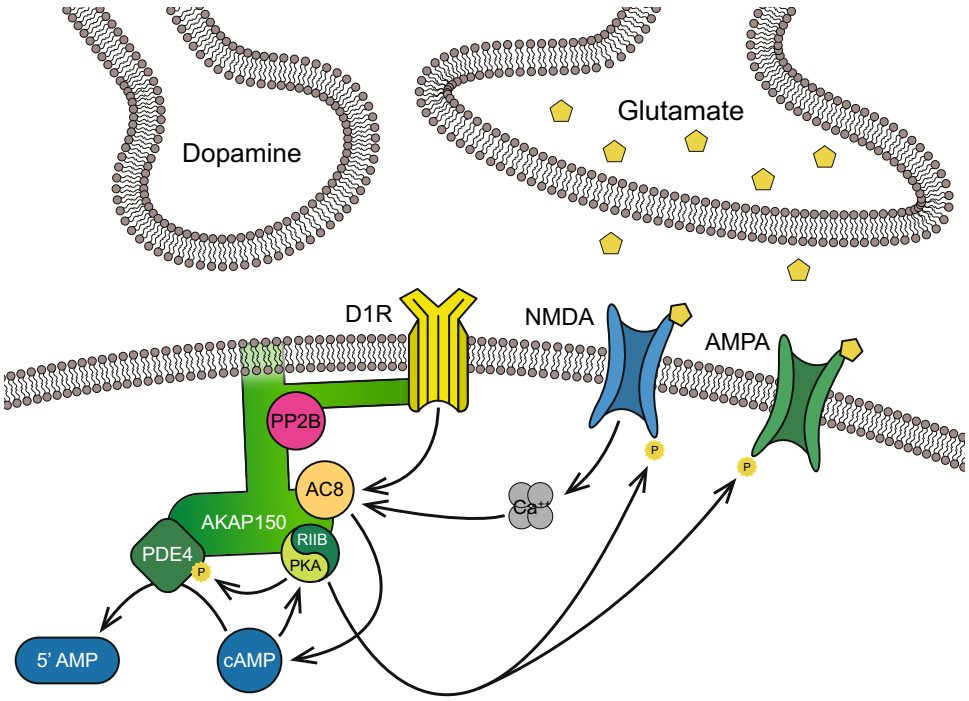

Fig. 8 Diagram illustrating important components of the cAMP cascade and their interactions in BLA synapses. Note the negative feedback loop whereby cAMP activates PKA, which enhances PDE4 activity, which in turn reduces cAMP concentration; this negative feedback loop is an essential component of compartmentalization

which phosphorylates PDE4, increasing its activity and activating a negative feedback mechanism which quickly returns cAMP levels to their basal state (Klussmann 2016). Elevated expression of AKAP150 has been linked to the formation of associative memories, and blocking the binding of AKAP150 and PDEs with the Ht31 molecule impairs LTP and learning, including the consolidation of fear memories (Huang et al. 2006; Nie et al. 2007; Nijholt et al. 2007; Moita et al. 2004). PDE4 is also implicated in contributing to the β-arrestin-mediated switching of β-adrenergic signaling from G_s-coupled to G_i-coupled, which may be of great importance in the amygdala, considering the critical role β-adrenergic signaling plays in fear memory formation (McGaugh and Roozendaal 2002). Finally, cAMP is further implicated in the formation of fear memory through its activation of cAMP Response Element Binding protein (CREB). In the basolateral amygdala, fear memories are stored in an ensemble of neurons defined by their elevated expression of CREB during memory acquisition, and later ablation of these neurons can erase the memory [Josselyn 2010].

This study represents a major step forward in understanding the molecular and physiological response to chronic stress. Much remains to be learned about which specific connections are being remodeled in response to stress and about the dynamic response of PDE4 expression and activity to stress exposure. A fuller understanding of the topography of connectivity in BLA principal neurons will better allow us to evaluate the significance of the morphological changes we have observed. Based on our findings, and on the highly dynamic nature of PDE4's role in memory formation, we suggest that more study is needed to understand the dynamic role of PDE4 in mediating the stress response before effective therapies can be developed.

Compliance with ethical standards

Funding This work was supported by funding from the National Institute of Mental Health, Grant MH069852 to DGR.

References

Abercrombie HC, Schaefer SM, Larson CL, Oakes TR, Lindgren KA et al (1998) Metabolic rate in the right amygdala predicts negative affect in depressed patients. Neuroreport 9:3301–3307

Baillie GS, Houslay MD (2005) Arrestin times for compartmentalised cAMP signalling and phosphodiesterase-4 enzymes. Curr Opin Cel Biol 17(2):129–134

Beylin AV, Shors TJ (1998) Stress enhances excitatory trace eyeblink conditioning and opposes acquisition of inhibitory conditioning. Behav Neurosci 112:1327–1338

Blair HT, Schafe GE, Bauer EP, Rodrigues SM, LeDoux JE (2001) Synaptic plasticity in the lateral amygdala: a cellular hypothesis of fear conditioning. Learn Mem 8:229–242

Blitzer RD, Wong T, Nouranifar R, Iyengar R, Landau EM (1995) Postsynaptic cAMP pathway gates early LTP in hippocampal CA1 region. Neuron 15:1403–1414

Blitzer RD, Connor JH, Brown GP, Wong T, Shenolikar S et al (1998) Gating of CaMKII by cAMP-regulated protein phosphatase activity during LTP. Science 280:1940–1942

Braga MF, Aroniadou-Anderjaska V, Li H (2004) The physiological role of kainate receptors in the amygdala. Mol Neurobiol 30:127–141

Brown SM, Henning S, Wellman CL (2005) Mild, short-term stress alters dendritic morphology in rat medial prefrontal cortex. Cereb Cortex 15(11):1714–1722

Bureau Y, Handa M, Zhu Y, Laliberte F, Moore CS, Liu S, Huang Z, MacDonald D, Xu DG, Robertson GS (2006) Neuroanatomical and pharmacological assessment of Fos expression induced in the rat brain by the phosphodiesterase-4 inhibitor 6-(4-pyridylmethyl)-8-(3-nitrophenyl) quinoline. Neuropharmacology 51(5):974–985

Caudal D, Godsil BP, Mailliet F, Bergerot D, Jay TM (2010) Acute stress induces contrasting changes in AMPA receptor subunit phosphorylation within the prefrontal cortex, amygdala and hippocampus. PLoS One 5:e15282

Chen CC, Yang CH, Huang CC, Hsu KS (2010) Acute stress impairs hippocampal mossy fiber-CA3 long-term potentiation by enhancing cAMP-specific phosphodiesterase 4 activity. Neuropsychopharmacology 35(7):1605–1617

Conrad CD, LeDoux JE, Magariños AM, McEwen BS (1999) Repeated restraint stress facilitates fear conditioning independently of causing hippocampal CA3 dendritic atrophy. Behav Neurosci 113(5):902–913

Cook SC, Wellman CL (2004) Chronic stress alters dendritic morphology in rat medial prefrontal cortex. J Neurobiol 60(2):236–248

Cordero MI, Venero C, Kruyt ND, Sandi C (2003) Prior exposure to a single stress session facilitates subsequent contextual fear conditioning in rats. Evidence for a role of corticosterone. Horm Behav 44:338–345

Cui H, Sakamoto H, Higashi S, Kawata M (2008) Effects of single-prolonged stress on neurons and their afferent inputs in the amygdala. Neuroscience 152(3):703–712

Drevets WC (1999) Prefrontal cortical-amygdalar metabolism in major depression. Ann N Y Acad Sci 877:614–637

Ehrlich DE, Rainnie DG (2015) Prenatal stress alters the development of socioemotional behavior and amygdala neuron excitability in rats. Neuropsychopharmacology 40(9):2135–2145

Ehrlich DE, Ryan SJ, Rainnie DG (2012) Postnatal development of electrophysiological properties of principal neurons in the rat basolateral amygdala. J Physiol 590(19):4819–4838

Hazra R, Guo JD, Dabrowska J, Rainnie DG (2012) Differential distribution of serotonin receptor subtypes in BNST(ALG) neurons: modulation by unpredictable shock stress. Neuroscience 225:9–21

Huang T, McDonough CB, Abel T (2006) Compartmentalized PKA signaling events are required for synaptic tagging and capture during hippocampal late-phase long-term potentiation. Eur J Cell Biol 85(7):635–642

Hubert GW, Li C, Rainnie DG, Muly EC (2014) Effects of stress on AMPA receptor distribution and function in the basolateral amygdala. Brain Struct Funct 219(4):1169–1179

Itoh T, Abe K, Tokumura M, Horiuchi M, Inoue O, Ibii N (2003) Different regulation of adenylyl cyclase and rolipram-sensitive phosphodiesterase activity on the frontal cortex and hippocampus in learned helplessness rats. Brain Res 991(1–2):142–149

Josselyn SA (2010) Continuing the search for the engram: examining the mechanism of fear memories. J Psychiatry Neurosci 35(4):221–228

Kavushansky A, Richter-Levin G (2006) Effects of stress and corticosterone on activity and plasticity in the amygdala. J Neurosci Res 84(7):1580–1587

Klussmann E (2016) Protein-protein interactions of PDE4 family members - Functions, interactions and therapeutic value. Cell Signal 28(7):713–718

LeDoux JE (1993) Emotional memory systems in the brain. Behav Brain Res 58:69–79

Li X, Baillie GS, Houslay MD (2009) Mdm2 directs the ubiquitination of beta-arrestin-sequestered cAMP phosphodiesterase-4D5. J Biol Chem 284(24):16170–16182

Li C, Dabrowska J, Hazra R, Rainnie DG (2011) Synergistic activation of dopamine D1 and TrkB receptors mediate gain control of synaptic plasticity in the basolateral amygdala. PLoS One 6:e26065

Liu RJ, Aghajanian GK (2008) Stress blunts serotonin- and hypocretin-evoked EPSCs in prefrontal cortex: role of corticosterone-mediated apical dendritic atrophy. Proc Natl Acad Sci USA 105(1):359–364

Livak KJ, Schmittgen TD (2001) Analysis of relative gene expression data using real-time quantitative PCR and the 2(-Delta Delta C(T)) method. Methods 25(4):402–408

McEwen BS (2005) Glucocorticoids, depression, and mood disorders: structural remodeling in the brain. Metabolism 54(5 Suppl 1):20–23

McGaugh JL, Roozendaal B (2002) Role of adrenal stress hormones in forming lasting memories in the brain. Curr Opin Neurobiol 12(2):205–210

McGirr A, Lipina TV, Mun HS, Georgiou J, Al-Miri AH, Ng E, Zhai D, Elliot C, Cameron RT, Mullings JG, Liu F, Baillie GS, Clapcote SJ, Roder JD (2016) Specific inhibition of phosphodiesterase-4B results in anxiolysis and facilitates memory acquisition. Neuropsychopharmacology 41(4):1080–1092

Migaud M, Charlesworth P, Dempster M, Webster LC, Watabe AM, Makhinson M, He Y, Ramsay MF, Morris RG, Morrison JH, O'Dell TJ, Grant SG (1998) Enhanced long-term potentiation and impaired learning in mice with mutant postsynaptic density-95 protein. Nature 396(6710):433–439

Mitra R, Jadhav S, McEwen BS, Vyas A, Chattarji S (2005) Stress duration modulates the spatiotemporal patterns of spine formation in the basolateral amygdala. Proc Natl Acad Sci USA 102:9371–9376

Moberg CA, Curtin JJ (2009) Alcohol selectively reduces anxiety but not fear: startle response during unpredictable versus predictable threat. J Abnorm Psychol 118(2):335–347

Moench KM, Maroun M, Kavushansky A, Wellman C (2015) Alterations in neuronal morphology in infralimbic cortex predict resistance to fear extinction following acute stress. Neurobiol Stress 3:23–33

Moita MA, Rosis S, Zhou Y, LeDoux JE, Blair HT (2004) Putting fear in its place: remapping of hippocampal place cells during fear conditioning. J Neurosci 2004 Aug 4 24(31):7015–7023

Nie T, McDonough CB, Huang T, Nguyen PV, Abel T (2007) Genetic disruption of protein kinase A anchoring reveals a role for compartmentalized kinase signaling in theta-burst long-term potentiation and spatial memory. J Neurosci 27(38):10278–10288

Nijholt IM, Ostroveanu A, de Bruyn M, Luiten PG, Eisel UL, Van der Zee EA (2007) Both exposure to a novel context and associative learning induce an upregulation of AKAP150 protein in mouse hippocampus. Neurobiol Learn Mem 87(4):693–696

Otmakhova NA, Otmakhov N, Mortenson LH, Lisman JE (2000) Inhibition of the cAMP pathway decreases early long-term potentiation at CA1 hippocampal synapses. J Neurosci 20:4446–4451

Padival M, Quinette D, Rosenkranz JA (2013) Effects of repeated stress on excitatory drive of basal amygdala neurons in vivo. Neuropsychopharmacology 38(9):1748–1762

Pickel VM, Colago EE, Mania I, Molosh AI, Rainnie DG (2006) Dopamine D1 receptors co-distribute with *N*-methyl-$_D$-aspartic acid type-1 subunits and modulate synaptically-evoked *N*-methyl-$_D$-aspartic acid currents in rat basolateral amygdala. Neuroscience 142:671–690

Pillai AG, Anilkumar S, Chattarji S (2012) The same antidepressant elicits contrasting patterns of synaptic changes in the amygdala vs hippocampus. Neuropsychopharmacology 37(12):2702–2711

Radley JJ, Sisti HM, Hao J, Rocher AB, McCall T, Hof PR, McEwen BS, Morrison JH (2004) Chronic behavioral stress induces apical dendritic reorganization in pyramidal neurons of the medial prefrontal cortex. Neuroscience 2004;125(1):1–6

Rainnie DG (1999) Serotonergic modulation of neurotransmission in the rat basolateral amygdala. J Neurophysiol 82(1):69–85

Rainnie DG, Asprodini EK, Shinnick-Gallagher P (1993) Intracellular recordings from morphologically identified neurons of the basolateral amygdala. J Neurophysiol 69:1350–1362

Rau V, DeCola JP, Fanselow MS (2005) Stress-induced enhancement of fear learning: an animal model of posttraumatic stress disorder. Neurosci Biobehav Rev 29(8):1207–1223

Rauch SL, Whalen PJ, Shin LM, McInerney SC, Macklin ML et al (2000) Exaggerated amygdala response to masked facial stimuli in posttraumatic stress disorder: a functional MRI study. Biol Psychiatry 47:769–776

Reznikov LR, Grillo CA, Piroli GG, Pasumarthi RK, Reagan LP et al (2007) Acute stress-mediated increases in extracellular glutamate levels in the rat amygdala: differential effects of antidepressant treatment. Eur J Neurosci 25:3109–3114

Rodriguez Manzanares PA, Isoardi NA, Carrer HF, Molina VA (2005) Previous stress facilitates fear memory, attenuates GABAergic inhibition, and increases synaptic plasticity in the rat basolateral amygdala. J Neurosci 25:8725–8734

Rogan MT, Staubli UV, LeDoux JE (1997) Fear conditioning induces associative long-term potentiation in the amygdala. Nature 390:604–607

Rosenkranz JA, Venheim ER, Padival M (2010) Chronic stress causes amygdala hyperexcitability in rodents. Biol Psychiatry 67:1128–1136

Rutten K, Misner DL, Works M, Blokland A, Novak TJ et al (2008) Enhanced long-term potentiation and impaired learning in phosphodiesterase 4D-knockout (PDE4D) mice. Eur J Neurosci 28:625–632

Rutten K, Wallace TL, Works M, Prickaerts J, Blokland A, Novak TJ, Santarelli L, Misner DL (2011) Enhanced long-term depression and impaired reversal learning in phosphodiesterase 4B-knockout (PDE4B(-/-)) mice. Neuropharmacology 61:138–147

Ryan SJ, Ehrlich DE, Rainnie DG (2014) Morphology and dendritic maturation of developing principal neurons in the rat basolateral amygdala. Brain Struct Funct 221(2):839–854

Shors TJ, Foy MR, Levine S, Thompson RF (1990) Unpredictable and uncontrollable stress impairs neuronal plasticity in the rat hippocampus. Brain Res Bull 24(5):663–667

Shors TJ, Weiss C, Thompson RF (1992) Stress-induced facilitation of classical conditioning. Science 257:537–539

Sink KS, Walker DL, Yang Y, Davis M (2011) Calcitonin gene-related peptide in the bed nucleus of the stria terminalis produces an anxiety-like pattern of behavior and increases neural activation in anxiety-related structures. J Neurosci 31:1802–1810

Suvrathan A, Bennur S, Ghosh S, Tomar A, Anilkumar S, Chattarji S (2014) Stress enhances fear by forming new synapses with greater capacity for long-term potentiation in the amygdala. Philos Trans R Soc Lond B Biol Sci 369(1633)

Terrin A, Di Benedetto G, Pertegato V, Cheung YF, Baillie G, Lynch MJ, Elvassore N, Prinz A, Herberg FW, Houslay MD, Zaccolo M (2006) PGE(1) stimulation of HEK293 cells generates multiple contiguous domains with different [cAMP]:

role of compartmentalized phosphodiesterases. J Cell Biol 175(3):441–451

Tsai SF, Huang TY, Chang CY, Hsu YC, Chen SJ, Yu L, Kuo YM, Jen CJ (2014) Social instability stress differentially affects amygdalar neuron adaptations and memory performance in adolescent and adult rats. Front Behav Neurosci 8:27

Vandesompele J, De Preter K, Pattyn F, Poppe B, Van Roy N, De Paepe A, Speleman F (2002) Accurate normalization of real-time quantitative RT-PCR data by geometric averaging of multiple internal control genes. Genome Biol 3(7):RESEARCH0034

Villarreal G, King CY (2001) Brain imaging in posttraumatic stress disorder. Semin Clin Neuropsychiatry 6:131–145

Vouimba RM, Yaniv D, Diamond D, Richter-Levin G (2004) Effects of inescapable stress on LTP in the amygdala versus the dentate gyrus of freely behaving rats. Eur J Neurosci 19:1887–1894

Vyas A, Mitra R, Shankaranarayana Rao BS, Chattarji S (2002) Chronic stress induces contrasting patterns of dendritic remodeling in hippocampal and amygdaloid neurons. J Neurosci 22(15):6810–6818

Vyas A, Pillai AG, Chattarji S (2004) Recovery after chronic stress fails to reverse amygdaloid neuronal hypertrophy and enhanced anxiety-like behavior. Neuroscience 128(4):667–673

Vyas A, Jadhav S, Chattarji S (2006) Prolonged behavioral stress enhances synaptic connectivity in the basolateral amygdala. Neuroscience 143:387–393

Walker DL, Davis M (1997) Double dissociation between the involvement of the bed nucleus of the stria terminalis and the central nucleus of the amygdala in startle increases produced by conditioned versus unconditioned fear. J Neurosci 17:9375–9383

Walker DL, Toufexis DJ, Davis M (2003) Role of the bed nucleus of the stria terminalis versus the amygdala in fear, stress, and anxiety. Eur J Pharmacol 463(1–3):199–216

Watanabe Y, Gould E, McEwen BS (1992a) Stress induces atrophy of apical dendrites of hippocampal CA3 pyramidal neurons. Brain Res 588:341–345

Watanabe Y, Gould E, Daniels DC, Cameron H, McEwen BS (1992b) Tianeptine attenuates stress-induced morphological changes in the hippocampus. Eur J Pharmacol 222:157–162

Werenicz A, Christoff RR, Blank M, Jobim PF, Pedroso TR, Reolon GK, Schröder N, Roesler R (2012) Administration of the phosphodiesterase type 4 inhibitor rolipram into the amygdala at a specific time interval after learning increases recognition memory persistence. Learn Mem 19(10):495–498

Wood GE, Norris EH, Waters E, Stoldt JT, McEwen BS (2008) Chronic immobilization stress alters aspects of emotionality and associative learning in the rat. Behav Neurosci 122(2):282–292

Zhang HT, Huang Y, Masood A, Stolinski LR, Li Y, Zhang L, Dlaboga D, Jin SL, Conti M, O'Donnell JM (2008) Anxiogenic-like behavioral phenotype of mice deficient in phosphodiesterase 4B (PDE4B). Neuropsychopharmacology 33(7):1611–1623

Zhu D, Li C, Swanson AM, Villalba RM, Guo J, Zhang Z, Matheny S, Murakami T, Stephenson JR, Daniel S, Fukata M, Hall RA, Olson JJ, Neigh GN, Smith Y, Rainnie DG, Van Meir EG (2015) BAI1 regulates spatial learning and synaptic plasticity in the hippocampus. J Clin Invest. 125(4):1497–4508